Subdiffusion in a bounded domain with a partially absorbing-reflecting boundary

Denis S. Grebenkov*

Laboratoire de Physique de la Matière Condensée, C.N.R.S.–Ecole Polytechnique, 91128 Palaiseau, France

(Received 30 October 2009; revised manuscript received 15 January 2010; published 24 February 2010)

The exit time of a subdiffusive process from a bounded domain with a partially absorbing/reflecting boundary is considered. The short-time and long-time behaviors of the exit time probability density are investigated by using a spectral decomposition on the basis of the Laplace operator eigenfunctions. Rotation-invariant domains are analyzed in depth in order to illustrate the use of theoretical formulas and to compare them to numerical simulations. The asymptotic results obtained are relevant for describing subdiffusion inside a living cell with a semipermeable membrane, in a chemical reactor filled with catalytic grains of finite reactivity, or in mineral or biological samples which are probed by nuclear magnetic resonance measurements subject to surface relaxation.

DOI: 10.1103/PhysRevE.81.021128   PACS number(s): 02.50.−r, 05.60.−k, 05.10.−a

I. INTRODUCTION

Anomalous diffusion, for which the mean-square displacement of a particle grows sublinearly in time, $\langle[x(t)-x(0)]^2\rangle \propto t^{\alpha}$, became a generic feature of many complex systems. Examples can be found in various fields ranging from biophysics (e.g., transport of large molecules in living cells [1,2]), to geophysics and ecology (e.g., tracer diffusion in subsurface hydrology [3]). Crowding and caging, geometrical traps and energetic barriers, and many other mechanisms may lead to long-tailed waiting time distributions which result in a sublinear growth of the mean-square displacement [4–10].

In many practical situations, the dynamics is not only slowed down, but particles are restricted by a boundary of a confining domain. For example, a semipermeable cellular membrane englobes the content of a living cell (proteins, macromolecules, etc.) leaving a possibility for an exchange with the extracellular space [11–13]; a catalytic surface enables for arriving species to be chemically transformed [14–18]; an interface between solid/void phases in mineral samples and biological tissues causes surface relaxation in nuclear magnetic resonance (NMR) experiments [19]. The functioning of a biological system, the efficiency of a chemical reactor and the signal amplitude in an NMR measurement depend on *how long a particle remains inside a confining domain, before being transferred, chemically transformed or relaxed*.

Many theoretical, numerical and experimental studies concerned the first-passage time for normal diffusion [20–27]. Recently, several groups investigated this question for subdiffusion. Lua and Grosberg studied the first-passage times for a particle, executing one-dimensional diffusive and subdiffusive motions in an asymmetric sawtooth potential, to exit one of the boundaries [28]. Yuste and Linderberg computed the asymptotic survival probability of a spherical target in the presence of a single subdiffusive trap or surrounded by a sea of subdiffusive traps [29]. Condamin and co-workers derived a relationship between the moments of the first-passage time for normal diffusion and the first-passage time density for subdiffusive processes [30,31]. They gave explicit evaluation of the first-passage time distribution for general three-dimensional bounded domains, with a special focus on targer search problems. All these studies concerned the first-passage time when a subdiffusive process is stopped after the first encounter with a boundary (e.g., a target). Such a boundary is called "perfectly absorbing:" once a particle arrives onto the boundary, it is immediately transferred, reacted or relaxed, i.e., the corresponding surface permeability, reactivity or relaxivity is infinite.

We consider a more general case of partially absorbing/reflecting boundaries which are relevant for various applications [32–40]. Once a particle approached such a boundary, it may either interact with the boundary (via adsorption, transfer, chemical transformation, relaxation, etc.), or to be reflected back towards the bulk to continue its motion. Since the particle may not interact with the boundary at their first encounter, the particle would remain longer inside a confining domain. The focus is now not on the first-passage time, but on the last-passage time when a particle is finally transferred, reacted or relaxed with a *finite* permeability, reactivity or relaxivity. In biology, the last-passage time is equivalent to the exit time which describes how long a particle remains in a cell prior to its transfer through a semipermeable cellular membrane. In chemistry and NMR applications, the last-passage time is the moment when a species is chemically transformed or relaxed on the surface. In what follows, we shall speak about exit times, keeping in mind other interpretations of the last-passage time. How does the surface permeability influence the distribution of exit times? May the shape of a confining domain change this distribution? What is the role of the exponent α characterizing the subdiffusive process? The aim of the present paper is to answer these questions.

In Sec. II, the survival probability of a particle subdiffusing inside a bounded domain is calculated. The time derivative of the survival probability is the probability density of the exit time from the domain (the first-passage time appearing as a limiting case). The computation relies on a spectral decomposition of a subdiffusive propagator on the basis of the Laplace operator eigenfunctions. This general though formal representation allows one to separate time and space

*denis.grebenkov@polytechnique.edu

dependences. The short-time and long-time asymptotic behaviors of spectral decompositions are analyzed, with a special emphasis on comparison between normal diffusion ($\alpha=1$) and subdiffusion ($0<\alpha<1$). In Sec. III, explicit formulas for the exit time probability density are derived in the case of rotation-invariant (or spherical) domains. Numerical results are presented in Sec. IV for rotation-invariant and rectangular domains. The role of a finite permeability, reactivity or relaxivity is outlined and the consequences of the short-time behavior are discussed. Some technical details and further discussions are grouped in Appendixes.

II. GENERAL DOMAINS

A. Subdiffusive propagator

In the framework of continuous-time random walks (CTRWs) or fractional Fokker-Planck equation (FFPE), a subdiffusive process with an exponent $0<\alpha\le 1$ is described by a propagator $G_t^\alpha(\mathbf{r}_0,\mathbf{r})$ that is the probability for a particle which started from $\mathbf{r}_0$ at time 0 to be found in a vicinity of $\mathbf{r}$ at a later time t. In absence of external forces or fields, the time evolution of the propagator is governed by a fractional diffusion (or heat) equation [5,9],

$$\frac{\partial}{\partial t}G_t^\alpha(\mathbf{r}_0,\mathbf{r}) = D_\alpha\, {}_0D_t^{1-\alpha}\Delta_{\mathbf{r}}G_t^\alpha(\mathbf{r}_0,\mathbf{r}), \quad (1)$$

where $\Delta_{\mathbf{r}}\equiv\Delta\equiv\partial^2/\partial_1^2+\ldots+\partial^2/\partial_d^2$ is the d-dimensional Laplace operator, and D_α is a generalized diffusion coefficient (in units m^2/s^α). Memory effects of a subdiffusive process are introduced through the Riemann-Liouville fractional differential operator ${}_0D_t^{1-\alpha}$ [41,42],

$${}_0D_t^{1-\alpha}g(t) = \frac{1}{\Gamma(\alpha)}\frac{\partial}{\partial t}\int_0^t dt'\frac{g(t')}{(t-t')^{1-\alpha}}, \quad (2)$$

which is defined for any sufficiently well-behaved function $g(t)$ ($\Gamma(z)$ is the Gamma function). The evolution starts from a pointlike source at $\mathbf{r}_0$

$$G_{t=0}^\alpha(\mathbf{r}_0,\mathbf{r}) = \delta(\mathbf{r}-\mathbf{r}_0), \quad (3)$$

$\delta(\mathbf{r}-\mathbf{r}_0)$ being the Dirac distribution. It is worth noting that fractional diffusion equation is not unique model which results in a sublinear growth of the mean-square displacement. Fractional Brownian motion, normal diffusion on fractal sets and other mechanisms which may also yield "anomalous" (sublinear) diffusion, are not considered in this paper.

When the motion of a particle is restricted by a boundary $\partial\Omega$ of a diffusion-confining domain Ω, an appropriate boundary condition should be imposed. A partially absorbing/reflecting boundary is often described by Robin (also known as radiation, Fourier, third, etc.) boundary condition which is a linear combination of Dirichlet and Neumann boundary conditions [14,32–34],

$$\Lambda\frac{\partial}{\partial n}G_t^\alpha(\mathbf{r}_0,\mathbf{r}) + G_t^\alpha(\mathbf{r}_0,\mathbf{r}) = 0 \quad (\mathbf{r}\in\partial\Omega), \quad (4)$$

where Λ is a positive parameter, and $\partial/\partial n$ is the normal derivative on the boundary pointing towards the exterior of a confining domain. Eq. (4) is a form of a mass conservation law when the diffusive flux toward the boundary is equal to the flux across the boundary. Collins and Kimball introduced the Robin boundary condition in order to describe partially diffusion-controlled reactions [14], while Seki *et al.* [43] and later Eaves and Reichman [44] justified this condition for subdiffusion. The positive parameter Λ which is homogeneous to a length, is the ratio between the bulk and surface transport coefficients: $\Lambda=D_\alpha/W_\alpha$, W_α being the (generalized) surface permeability, relaxivity or reactivity (although Λ may depend on α, we keep writing Λ instead of Λ_α).

In the limiting case $\Lambda=0$, one retrieves Dirichlet boundary condition for a perfectly absorbing boundary. The opposite case of $\Lambda=\infty$ corresponds to Neumann boundary condition for a perfectly reflecting boundary. The length Λ controls the balance between these limits or, equivalently, the balance between absorptions and reflections. Although some more sophisticated boundary conditions may sometimes be required in order to describe surface exchange processes [45–47], our focus is specifically on Robin boundary condition (4).

For a bounded domain, a propagator $G_t^\alpha(\mathbf{r}_0,\mathbf{r})$ can be written in the form of a spectral decomposition [5]

$$G_t^\alpha(\mathbf{r}_0,\mathbf{r}) = \sum_{m=0}^{\infty}E_\alpha(-D_\alpha\lambda_m t^\alpha)u_m^*(\mathbf{r}_0)u_m(\mathbf{r}), \quad (5)$$

where the asterisk denotes a complex conjugate, and the Laplace operator eigenfunctions $u_m(\mathbf{r})$ and eigenvalues λ_m ($m=0,1,2,\ldots$) are defined as

$$\Delta u_m(\mathbf{r}) + \lambda_m u_m(\mathbf{r}) = 0 \quad (\mathbf{r}\in\Omega),$$

$$\Lambda\frac{\partial}{\partial n}u_m(\mathbf{r}) + u_m(\mathbf{r}) = 0 \quad (\mathbf{r}\in\partial\Omega). \quad (6)$$

The eigenvalues λ_m are positive and conventionally ordered: $0\le\lambda_0\le\lambda_1\le\lambda_2\le\ldots$, while the eigenfunctions $u_m(\mathbf{r})$ are orthonormal [48],

$$\int_\Omega d\mathbf{r}\, u_m^*(\mathbf{r})u_{m'}(\mathbf{r}) = \delta_{m,m'},$$

$\delta_{m,m'}$ being the Kronecker delta symbol.

The Mittag-Leffler function $E_\alpha(z)$ in Eq. (5) is defined either by a Taylor series [49],

$$E_\alpha(z) = \sum_{k=0}^{\infty}\frac{z^k}{\Gamma(\alpha k+1)},$$

or as a solution of the fractional differential equation,

$$-\frac{\partial}{\partial t}E_\alpha(-t^\alpha) = {}_0D_t^{1-\alpha}E_\alpha(-t^\alpha).$$

For $\alpha=1$, one gets $E_1(z)=e^z$, and Eq. (5) is a classical spectral decomposition of a propagator for normal diffusion,

$$G_t^1(\mathbf{r}_0,\mathbf{r}) = \sum_{m=0}^{\infty} e^{-D_1\lambda_m t} u_m^*(\mathbf{r}_0) u_m(\mathbf{r}). \quad (7)$$

Note that Eqs. (5) and (7) exhibit identical spatial dependences, in agreement with the fact that subdiffusion and diffusion can be related by changing a "time clock" (the operation known as "subordination" [50–55]).

B. Exit times

For a subdiffusive process with an exponent α, we denote T_α the exit time from a bounded domain Ω with a partially absorbing/reflecting boundary $\partial\Omega$. T_α is a random variable whose probability density $q_\alpha(\mathbf{r},t)$ depends on the shape of Ω, the starting point $\mathbf{r}$, the exponent α and the length Λ. We first consider the survival probability $Q_\alpha(\mathbf{r},t)$ that a particle which started from $\mathbf{r}$ at time 0 is survived until time t: $Q_\alpha(\mathbf{r},t)=\mathbb{P}\{T_\alpha > t\}$. The survival probability is simply the integral of a propagator $G_t^\alpha(\mathbf{r},\mathbf{r}')$ over the arrival points $\mathbf{r}' \in \Omega$. In turn, the probability density $q_\alpha(\mathbf{r},t)$ is the time derivative of $Q_\alpha(\mathbf{r},t)$,

$$q_\alpha(\mathbf{r},t) = -\frac{\partial}{\partial t} Q_\alpha(\mathbf{r},t) = \int_\Omega d\mathbf{r}' \left(-\frac{\partial}{\partial t} G_t^\alpha(\mathbf{r},\mathbf{r}')\right). \quad (8)$$

The spectral decomposition (5) yields

$$q_\alpha(\mathbf{r},t) = \sum_{m=0}^{\infty} \left(-\frac{\partial}{\partial t} E_\alpha(-D_\alpha \lambda_m t^\alpha)\right) u_m^*(\mathbf{r}) \int_\Omega d\mathbf{r}' u_m(\mathbf{r}'). \quad (9)$$

This is a general, though formal, spectral decomposition for the exit time probability density. The main advantage of Eq. (9) is that the dependences on the time t, the exponent α, and the starting point $\mathbf{r}$ are separate. For instance, the dependence on the starting point $\mathbf{r}$ is represented by the same eigenfunctions $u_m(\mathbf{r})$ for all subdiffusive processes (any α between 0 and 1, including normal diffusion with $\alpha=1$). These eigenfunctions enter in Eq. (9) with different "weights" depending on α.

C. Exit times for normal diffusion

For normal diffusion ($\alpha=1$), Eq. (9) becomes

$$q_1(\mathbf{r},t) = \sum_{m=0}^{\infty} e^{-D_1\lambda_m t} D_1 \lambda_m u_m^*(\mathbf{r}) \int_\Omega d\mathbf{r}' u_m(\mathbf{r}'). \quad (10)$$

This explicit formula yields spectral decompositions for all the moments of the exit time T_1,

$$\begin{aligned} \tau_\Omega^{(k)}(\mathbf{r}) &\equiv \mathbb{E}\{T_1^k\} \\ &\equiv \int_0^\infty dt\, t^k q_1(\mathbf{r},t) \\ &= k! \sum_{m=0}^{\infty} \frac{u_m(\mathbf{r})}{(D_1\lambda_m)^k} \int_\Omega d\mathbf{r}' u_m(\mathbf{r}'). \end{aligned} \quad (11)$$

For instance, the mean exit time $\tau_\Omega^{(1)}(\mathbf{r})$ characterizes how long, on average, Brownian motion started from $\mathbf{r}$ spends inside a domain Ω until the exit by a transfer through the boundary $\partial\Omega$. The spectral representation (11) allows one to write a set of Poisson equations for the moments [56]

$$\Delta \tau_\Omega^{(k)}(\mathbf{r}) + \frac{k}{D_1} \tau_\Omega^{(k-1)}(\mathbf{r}) = 0 \quad (\mathbf{r} \in \Omega),$$

$$\Lambda \frac{\partial}{\partial n} \tau_\Omega^{(k)}(\mathbf{r}) + \tau_\Omega^{(k)}(\mathbf{r}) = 0 \quad (\mathbf{r} \in \partial\Omega). \quad (12)$$

For rotation-invariant domains, $\Omega=\{\mathbf{r}\in\mathbb{R}^d : |\mathbf{r}| < R\}$, Eqs. (12) can be explicitly solved (see Appendix A), e.g.,

$$\tau_\Omega^{(1)}(\mathbf{r}) = \frac{R^2 - |\mathbf{r}|^2 + 2\Lambda R}{2dD_1}.$$

The mean exit time linearly increases with the length Λ which represents a finite permeability, reactivity or relaxivity of the boundary.

D. Long-time asymptotic behavior

For normal diffusion ($\alpha=1$), the long-time behavior of the probability density $q_1(\mathbf{r},t)$ is dominated by the ground eigenstate with the smallest eigenvalue λ_0,

$$q_1(\mathbf{r},t) \simeq e^{-D_1\lambda_0 t} D_1 \lambda_0 u_0^*(\mathbf{r}) \int_\Omega d\mathbf{r}' u_0(\mathbf{r}') \quad (t \to \infty) \quad (13)$$

[since $\lambda_0 < \lambda_1 \le \lambda_2 \le \ldots$, the other terms in Eq. (10) are exponentially small]. The smallest eigenvalue λ_0 fixes a characteristic time $(D\lambda_0)^{-1}$ of the exponential decay, or "lifetime" of the ground eigenmode. The corresponding eigenfunction $u_0^*(\mathbf{r})$ describes the dependence on the starting point $\mathbf{r}$.

For subdiffusion ($\alpha<1$), the situation is different. The long-time asymptotic behavior of the Mittag-Leffler functions with $0<\alpha<1$ is

$$E_\alpha(-t^\alpha) \simeq \sum_{k=1}^{\infty} \frac{(-1)^{k-1} t^{-\alpha k}}{\Gamma(1-\alpha k)} \quad (t \to \infty), \quad (14)$$

from which one deduces the long-time asymptotic behavior of a subdiffusive propagator with $0<\alpha<1$

$$G_t^\alpha(\mathbf{r}_0,\mathbf{r}) \simeq \sum_{k=1}^{\infty} \left[\frac{(-1)^{k-1}}{\Gamma(1-\alpha k)} \left(\frac{D_1}{D_\alpha}\right)^k t^{-\alpha k} \sum_{m=0}^{\infty} \frac{u_m^*(\mathbf{r}_0) u_m(\mathbf{r})}{(D_1\lambda_m)^k}\right] \quad (t \to \infty). \quad (15)$$

Note that this formula does not hold for $\alpha=1$. Using Eq. (8), one gets the long-time asymptotic behavior of the density $q_\alpha(\mathbf{r},t)$ with $0<\alpha<1$,

$$q_\alpha(\mathbf{r},t) \simeq \sum_{k=1}^{\infty} \frac{(-1)^k}{\Gamma(-\alpha k) k!} \left(\frac{D_1}{D_\alpha}\right)^k \frac{\tau_\Omega^{(k)}(\mathbf{r})}{t^{\alpha k+1}} \quad (t \to \infty). \quad (16)$$

A similar asymptotic result was derived by Condamin and co-workers for first-passage times [30]. A finite permeability, reactivity or relaxivity of the boundary enters uniquely through the moments $\tau_\Omega^{(k)}(\mathbf{r})$ for normal diffusion. The leading asymptotic term is

$$q_\alpha(\mathbf{r},t) \simeq \frac{\tau_\Omega^{(1)}(\mathbf{r})}{|\Gamma(-\alpha)|}\frac{D_1}{D_\alpha}t^{-\alpha-1} \quad (t\to\infty). \tag{17}$$

Although the mean exit time $\mathbb{E}\{T_\alpha\}$ for subdiffusion diverges, $\tau_\Omega^{(1)}(\mathbf{r})$ plays the role of a natural time scale for subdiffusion inside a given domain Ω.

We outline two apparent distinctions between Eqs. (13) and (17). First, an expected power-law decay of the density $q_\alpha(\mathbf{r},t)$ replaces the exponential one for $q_1(\mathbf{r},t)$. Second, a slower dynamics of subdiffusive particles implies that all the eigenfunctions $u_m(\mathbf{r})$ do determine the dependence of $q_\alpha(\mathbf{r},t)$ on the starting point $\mathbf{r}$ (instead of the single eigenfunction $u_0(\mathbf{r})$ for normal diffusion). The spatial dependence is represented through the mean exit time $\tau_\Omega^{(1)}(\mathbf{r})$ which is a universal characteristics of a confining domain Ω, regardless of the exponent α.

E. Uniform starting points

If the starting point is uniformly distributed over the domain, the averaged exit time probability density is

$$\langle q_\alpha(t)\rangle \equiv \frac{1}{V}\int_\Omega d\mathbf{r}\, q_\alpha(\mathbf{r},t) = \sum_{m=0}^{\infty}\left[-\frac{\partial}{\partial t}E_\alpha(-D_\alpha\lambda_m t^\alpha)\right]\frac{1}{V}\left[\int_\Omega d\mathbf{r}\, u_m(\mathbf{r})\right]^2,$$

V being the volume of Ω. The long-time asymptotic behavior is deduced from Eq. (14),

$$\langle q_\alpha(t)\rangle \simeq \sum_{k=1}^{\infty}\frac{(-1)^k t^{-\alpha k-1}}{\Gamma(-\alpha k)k!}\left(\frac{D_1}{D_\alpha}\right)^k\langle\tau_\Omega^{(k)}\rangle, \tag{18}$$

with the averaged moments $\langle\tau_\Omega^{(k)}\rangle$ of the exit time for normal diffusion,

$$\langle\tau_\Omega^{(k)}\rangle \equiv \frac{1}{V}\int_\Omega d\mathbf{r}\,\tau_\Omega^{(k)}(\mathbf{r}) = k!\sum_{m=0}^{\infty}(D_1\lambda_m)^{-k}\frac{1}{V}\left[\int_\Omega d\mathbf{r}\,u_m(\mathbf{r})\right]^2.$$

For rotation-invariant domains, we derived an explicit formula for the averaged moments in Appendix A.

F. Laplace-transformed densities

Once the Laplace operator eigenfunctions are known for a given domain Ω, the spectral decomposition (9) allows one to compute the probability density $q_\alpha(\mathbf{r},t)$. The major difficulty of spectral decompositions emerges in the short-time limit $t\to 0$ when a very large number of eigenfunctions is required for an accurate computation (see Sec. IV). This difficulty is particularly significant for subdiffusion because the Mittag-Leffler functions $E_\alpha(-z)$ with $0<\alpha<1$ exhibit a slow power-law decay (14). For this reason, the Laplace transform $\mathcal{L}$ of the probability density $q_\alpha(\mathbf{r},t)$ is often considered,

$$\tilde{q}_\alpha(\mathbf{r},s) \equiv \mathcal{L}[q_\alpha(\mathbf{r},t)](s) \equiv \int_0^\infty dt\, e^{-ts}q_\alpha(\mathbf{r},t).$$

Since the fractional derivative in Eq. (2) has a form of a convolution, its Laplace transform is simply the product of two Laplace transforms, namely, $\mathcal{L}[{}_0D_t^{1-\alpha}g(t)](s) = s^{1-\alpha}\mathcal{L}[g(t)](s)$. A fractional diffusion equation for $q_\alpha(\mathbf{r},t)$ is therefore reduced to a Helmholtz equation for $\tilde{q}_\alpha(\mathbf{r},s)$. In fact, the Laplace transform of Eq. (8) yields

$$\tilde{q}_\alpha(\mathbf{r},s) = 1 - s\mathcal{L}\left[\int_\Omega d\mathbf{r}' G_t^\alpha(\mathbf{r},\mathbf{r}')\right](s)$$

that allows one to write a Helmholtz equation for $\tilde{q}_\alpha(\mathbf{r},s)$,

$$s^\alpha\tilde{q}_\alpha(\mathbf{r},s) - D_\alpha\Delta\tilde{q}_\alpha(\mathbf{r},s) = 0 \quad (\mathbf{r}\in\Omega), \tag{19}$$

$$\Lambda\frac{\partial}{\partial n}\tilde{q}_\alpha(\mathbf{r},s) + \tilde{q}_\alpha(\mathbf{r},s) = 1 \quad (\mathbf{r}\in\partial\Omega). \tag{20}$$

Note that the factor s^α appears as a fixed parameter in the Helmholtz equation. As a consequence, its solution for subdiffusion $(0<\alpha<1)$ can be directly derived from the solution for normal diffusion $(\alpha=1)$ by substituting s/D_1 by s^α/D_α. This is an example of "subordination" meaning that diffusion and subdiffusion differ only by "time clocks," the difference being expressed through s^α/D_α in Laplace space. The analysis of the exit time T_α for a subdiffusive process is therefore fully reduced to "rescaling" of the same characteristics for normal diffusion. On one hand, one can readily use numerous analytical results about exit times known for normal diffusion [57]. On the other hand, fast random walk algorithms which were implemented for computing exit times for normal diffusion in complex geometries (e.g., see [23,58–62]), can potentially be adapted for subdiffusion.

Once a solution of Eqs. (19) and (20) is found, analytically or numerically, one can formally apply the inverse Laplace transform in order to retrieve the exit time probability density $q_\alpha(\mathbf{r},t)$. However, such a computation is technically difficult and rarely employed. In practice, one uses the asymptotic properties of the Laplace transform $\tilde{q}_\alpha(\mathbf{r},s)$ in the limit of s going to infinity in order to determine the short-time asymptotic behavior of $q_\alpha(\mathbf{r},t)$ (e.g., see [40,63]). In the next section, we illustrate this technique in the case of rotation-invariant domains.

III. ROTATION-INVARIANT DOMAINS

For rotation-invariant domains, $\Omega=\{\mathbf{r}\in\mathbb{R}^d : |\mathbf{r}|<R\}$, Eq. (19) is reduced to a modified Bessel equation

$$g''(z) + \frac{d-1}{z}g'(z) - g(z) = 0,$$

where $g(z)\equiv\tilde{q}_\alpha(\mathbf{r},s)$ and $z\equiv|\mathbf{r}|\sqrt{s^\alpha/D_\alpha}$. A regular solution of this equation satisfying the Robin boundary condition (20) is

$$\tilde{q}_\alpha(\mathbf{r},s) = \left(\frac{|\mathbf{r}|}{R}\right)^{1-d/2}\frac{I_{d/2-1}(|\mathbf{r}|\sqrt{s^\alpha/D_\alpha})}{W_d(s)}, \tag{21}$$

with

$$W_d(s) = I_{d/2-1}\left(R\sqrt{s^\alpha/D_\alpha}\right) + \Lambda\sqrt{s^\alpha/D_\alpha}I_{d/2}\left(R\sqrt{s^\alpha/D_\alpha}\right), \tag{22}$$

where $I_\nu(z)$ is the modified Bessel function of the first kind. It is worth noting that a solution of the exterior problem describing the probability density for target search times has a similar form, in which $I_{d/2-1}(z)$ and $I_{d/2}(z)$ are replaced by the modified Bessel functions $K_{d/2-1}(z)$ and $K_{d/2-1}(z)$ of the second kind [64]. For a perfectly absorbing boundary ($\Lambda=0$), one retrieves the results from Ref. [29].

A. Short-time asymptotic behavior

The asymptotic behavior of the Laplace transform $\tilde{q}_\alpha(\mathbf{r},s)$ as s goes to infinity allows one to investigate the short-time asymptotic behavior of the exit time probability density $q_\alpha(\mathbf{r},t)$. When $|\mathbf{r}|>0$, one gets as $s\to\infty$

$$\tilde{q}_\alpha(\mathbf{r},s) \simeq \left(\frac{|\mathbf{r}|}{R}\right)^{(1-d)/2} \frac{\exp[-(R-|\mathbf{r}|)\sqrt{s^\alpha/D_\alpha}]}{1+\frac{1-d^2}{8}\frac{\Lambda}{R}+\Lambda\sqrt{s^\alpha/D_\alpha}} \tag{23}$$

(the case $|\mathbf{r}|=0$ and related questions are discussed in Appendix B). Interestingly, the asymptotic behavior is different for a perfectly absorbing boundary ($\Lambda=0$) and for a partially absorbing boundary ($\Lambda>0$). Using Eq. (C5) from Appendix C, the short-time asymptotic behavior of the probability density $q_\alpha(\mathbf{r},t)$ is deduced in these two cases,

$$q_\alpha(\mathbf{r},t) \simeq t^{-1}\left(\frac{|\mathbf{r}|}{R}\right)^{(1-d)/2} q_\alpha^{(0)}\left(\left[\frac{(R-|\mathbf{r}|)^2\alpha^\alpha}{4D_\alpha t^\alpha}\right]^{1/(2-\alpha)}, \frac{\sqrt{D_\alpha t^\alpha}}{\Lambda}\right), \tag{24}$$

where

$$q_\alpha^{(0)}(z,y) = \frac{e^{-(2-\alpha)z}}{\sqrt{\pi(2-\alpha)}}\begin{cases}(\alpha z)^{1/2} & (y=\infty),\\ (\alpha z)^{(1-\alpha)/2}y & (y<\infty).\end{cases} \tag{25}$$

In both cases, the asymptotic behavior is dominated by the exponential factor $e^{-(2-\alpha)z}$ that makes the probability density decreasing very rapidly when t goes to 0.

For arbitrary bounded domain Ω (not necessarily rotation invariant), it is convenient to represent the probability density $q_\alpha(\mathbf{r},t)$ as

$$q_\alpha(\mathbf{r},t) = t^{-1}f_\alpha(\mathbf{r},t)q_\alpha^{(0)}\left(\left[\frac{|\mathbf{r}-\partial\Omega|^2\alpha^\alpha}{4D_\alpha t^\alpha}\right]^{1/(2-\alpha)}, \frac{\sqrt{D_\alpha t^\alpha}}{\Lambda}\right), \tag{26}$$

where $\delta=|\mathbf{r}-\partial\Omega|$ is the distance from the starting point $\mathbf{r}$ to the boundary $\partial\Omega$, and $f_\alpha(\mathbf{r},t)$ is a nonuniversal function which depends on the shape of Ω. We guess that the dependence of the function $f_\alpha(\mathbf{r},t)$ on time t cannot be stronger than a power law in the short-time limit. In other words, the function $f_\alpha(\mathbf{r},t)$ is expected to be a correction prefactor to the dominating exponential behavior through the universal function $q_\alpha^{(0)}(z,y)$. In the short-time limit, rare particles can reach the boundary, and these particles most probably arrive at the boundary points which are the nearest to the starting point. This argument qualitatively explains the presence of the distance to the boundary. A rigorous proof of this statement is a challenging problem. The following argument could be a first step toward such a proof.

Since subdiffusion is a continuous process, a particle started from a point $\mathbf{r}$ inside a bounded domain Ω can reach the boundary $\partial\Omega$ of this domain only after having intersected the sphere of radius $\delta=|\mathbf{r}-\partial\Omega|$ which is centered at $\mathbf{r}$. In other words, the exit time T_α from the domain Ω is always larger than the exit time T'_α from the inscribed sphere (the prime will denote the variables for the inscribed sphere). In probabilistic language, it means that $Q_\alpha(\mathbf{r},t)\geq Q'_\alpha(\mathbf{r},t)$ for all times $t>0$. Since $Q_\alpha(\mathbf{r},0)=Q'_\alpha(\mathbf{r},0)=1$ and both functions are smooth, the corresponding probability densities $q_\alpha(\mathbf{r},t)$ and $q'_\alpha(\mathbf{r},t)$ satisfy the inequality $q_\alpha(\mathbf{r},t)\leq q'_\alpha(\mathbf{r},t)$ for small enough times t. But the short-time asymptotic behavior of the probability density $q'_\alpha(\mathbf{r},t)$ for a sphere is given by Eq. (24) with $\Lambda=0$ (as we consider the first intersection with the inscribed sphere). This is an upper bound for the probability density $q_\alpha(\mathbf{r},t)$ for any bounded domain. Although this upper bound does not prove the conjectured asymptotic behavior of $q_\alpha(\mathbf{r},t)$, it gives a strong argument in favor of the dominating exponential factor in Eq. (24) for any bounded domain.

In many cases, the correction prefactor $f_\alpha(\mathbf{r},t)$ is simply independent of time. For instance, we saw in Eq. (24) that $f_\alpha(\mathbf{r},t)=(|\mathbf{r}|/R)^{(1-d)/2}$ (with $|\mathbf{r}|>0$) for rotation-invariant domains. In Sec. IV C, we compute numerically the function $f_\alpha(\mathbf{r},t)$ for rectangular domains and show that it is equal to 1 for most starting points. At the same time, Eq. (B2) from Appendix B provides an explicit example of a power-law dependence of the function $f_\alpha(\mathbf{r},t)$ on time. More generally, one may expect that the fractal dimension of an irregular boundary would modify the exponent of the power-law time dependence of $f_\alpha(\mathbf{r},t)$. An accurate numerical determination of this function for irregularly shaped domains is as well a challenging problem.

B. Uniform starting point

If the starting point $\mathbf{r}$ is chosen randomly with a uniform density, one gets

$$\langle\tilde{q}_\alpha(s)\rangle \equiv \frac{1}{V}\int_\Omega d\mathbf{r}\,\tilde{q}_\alpha(\mathbf{r},s) = \frac{d}{W_d(s)}\frac{I_{d/2}(R\sqrt{s^\alpha/D_\alpha})}{R\sqrt{s^\alpha/D_\alpha}}.$$

As earlier, the asymptotic behavior of $\langle\tilde{q}_\alpha(s)\rangle$ as s going to infinity is different for $\Lambda=0$ and $\Lambda>0$,

$$\langle\tilde{q}_\alpha(s)\rangle \simeq \begin{cases} d\frac{\sqrt{D_\alpha}}{R}s^{-\alpha/2} & (\Lambda=0)\\ d\frac{D_\alpha}{\Lambda R}s^{-\alpha} & (\Lambda>0),\end{cases}$$

from which the short-time asymptotic behavior of the averaged exit time probability density is deduced

$$\langle q_\alpha(t)\rangle \simeq \begin{cases} \dfrac{1}{\Gamma(\alpha/2)}\dfrac{d}{R}\sqrt{D_\alpha}t^{\alpha/2-1} & (\Lambda=0) \\ \dfrac{1}{\Gamma(\alpha)}\dfrac{d}{R}\dfrac{D_\alpha}{\Lambda}t^{\alpha-1} & (\Lambda>0). \end{cases} \quad (27)$$

In Eq. (24) and (25), the distinction between two cases $\Lambda=0$ and $\Lambda>0$ was difficult to grasp because the asymptotic behavior was dominated by the exponential factor. In contrast, the averaging over the starting point eliminates the exponential factor and accentuates the power law in Eq. (27). Since the particles which started closely to the boundary reach it very fast, the averaged density $\langle q_\alpha(t)\rangle$ does not vanish (as it was the case for $q_\alpha(\mathbf{r},t)$), but diverges. This divergence is faster for a perfectly absorbing boundary ($\Lambda=0$) because less time is needed to exit from the domain. The difference between the exponent $\alpha/2-1$ for $\Lambda=0$ and the exponent $\alpha-1$ for $\Lambda>0$ can be used to distinguish these two regimes from fitting experimental or simulated data. As the assumption of infinite permeability, reactivity or relaxivity ($\Lambda=0$) is often not valid, experimental results should be interpreted carefully in the short-time limit. In particular, the use of the first relation in Eqs. (27) instead of the second one may lead to erroneous determination of the exponent α from fitting $\langle q_\alpha(t)\rangle$ versus t. It is worth noting that the second relation in Eqs. (27) allows one to determine the length Λ and to characterize the surface permeability.

Equation (27) was rigorously derived for rotation-invariant domains. The factor d/R can be interpreted as the surface-to-volume ratio S/V of these domains. For any bounded domain with a smooth boundary, the short-time asymptotic behavior is conjectured to be

$$\langle q_\alpha(t) > \simeq \begin{cases} \dfrac{1}{\Gamma(\alpha/2)}\dfrac{S}{V}\sqrt{D_\alpha}t^{\alpha/2-1} & (\Lambda=0) \\ \dfrac{1}{\Gamma(\alpha)}\dfrac{S}{V}\dfrac{D_\alpha}{\Lambda}t^{\alpha-1} & (\Lambda>0). \end{cases} \quad (28)$$

This behavior is well known for normal diffusion ($\alpha=1$). For subdiffusion, the valididity of these relations is checked numerically for rectangular domains in Sec. IV C.

IV. NUMERICAL RESULTS

In this section, we illustrate spectral decompositions and asymptotic results presented in previous sections. Although the results are applicable for any bounded domain, a sphere ($d=3$) is chosen as a typical example because of its relevance for biological applications (e.g., as a simplified model of a living cell). As the results for other rotation-invariant domains [interval in one dimension and disk in two dimensions] show similar features, they are not presented.

The Laplace operator eigenfunctions for a sphere are known explicitly [65,66] that makes a numerical computation of spectral decompositions straightforward (technical details can be found, e.g., in [40]). For progressively increasing eigenvalues λ_m, the Mittag-Leffler function in Eq. (5) and its derivative in Eq. (9) decrease with m. A truncated spectral decomposition with a finite number of terms allows

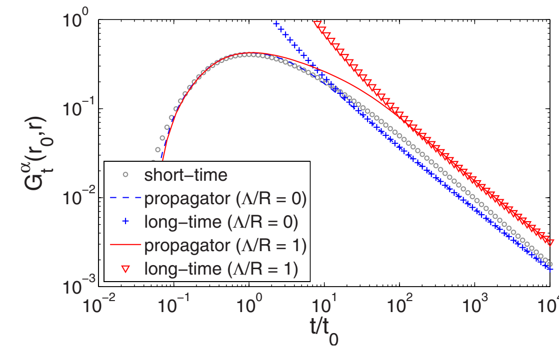

FIG. 1. (Color online) Subdiffusive propagator $G_t^\alpha(\mathbf{r}_0,\mathbf{r})$ for a sphere ($d=3$) with $\alpha=2/3$, $\mathbf{r}_0=0$, $|\mathbf{r}|=0.5R$, and two values $\Lambda=0$ (dashed blue line) and $\Lambda=R$ (solid red line). The time scale t_0 is given by Eq. (C7). Circles show the short-time approximation (C8), while crosses and triangles represent the long-time approximations (15) truncated to two terms, for $\Lambda=0$ and $\Lambda=R$, respectively.

a numerical computation with a desired accuracy. In the case of a sphere, 200 eigenmodes were used for computing spectral decompositions in the examples shown. The radius R of the sphere and the generalized diffusion coefficients D_α were set to 1.

The long-time asymptotic behavior [Eq. (15)] of the exit time probability density $q_\alpha(\mathbf{r},t)$ involves on the moments $\mathcal{T}_\Omega^{(k)}(\mathbf{r})$ for a sphere. Their computation is described in Appendix A (in practice, the set of linear equations (A3) was written in a matrix form and then solved numerically).

A. Subdiffusive propagator

Figure 1 shows the time dependence of the subdiffusive propagator $G_t^\alpha(\mathbf{r}_0,\mathbf{r})$ for a sphere ($d=3$), with $\alpha=2/3$ as an arbitrary example. The subdiffusive propagator exhibits a maximum at time t which is close to the time scale t_0 from Eq. (C7). This time scale, which is set by the distance between the points $\mathbf{r}_0$ and $\mathbf{r}$, is used to normalize the time t.

The asymptotic formula (C6) accurately approximates the subdiffusive propagator in the short-time limit, for both a perfectly absorbing boundary ($\Lambda=0$) and a partially absorbing boundary (with $\Lambda=R$ as an example). In the case presented, the starting point $\mathbf{r}_0=0$ and the arrival point $|\mathbf{r}|=0.5R$ are far from the boundary, so that the boundary condition (the value of Λ) is irrelevant. In fact, particles do not have enough time to "feel" the presence of a boundary in the short-time limit. A different behavior is expected when either of two points $\mathbf{r}_0$ and $\mathbf{r}$ (or both) is close to the boundary. There is a small discrepancy between the spectral decomposition (5) and the asymptotic formula (C6) at very small times ($t/t_0<0.01$). In this time range, the spectral decomposition of the propagator with 200 eigenmodes is inaccurate. In turn, the asymptotic formula (C6) is getting more and more accurate for smaller times, providing thus a way for evaluating the subdiffusive propagator in this case.

The asymptotic formula (15) truncated to two terms accurately approximates the subdiffusive propagator in the long-time limit. We checked that a single term was not enough for getting accurate results, while the use of three, four, etc. terms was not relevant in practice.

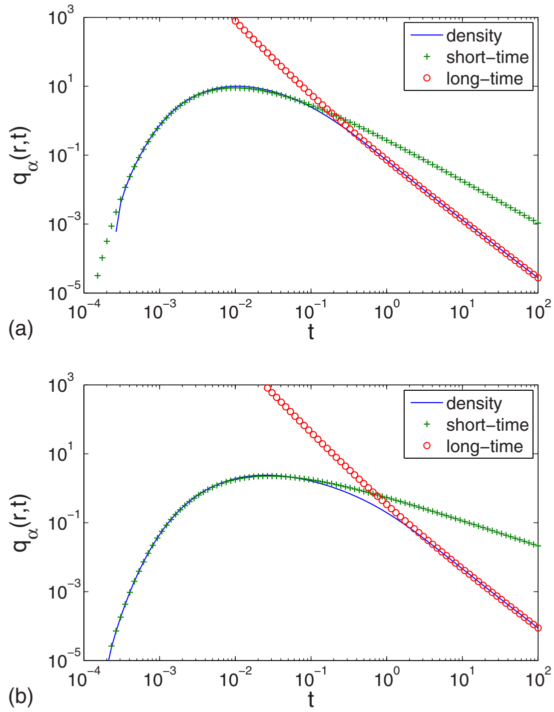

FIG. 2. (Color online) The exit time probability density $q_\alpha(\mathbf{r},t)$ for a sphere ($d=3$) with $\alpha=2/3$ and $|\mathbf{r}|=0.25R$ (top: $\Lambda=0$; bottom: $\Lambda=R$). Pluses and circles show respectively the short-time approximation (24) and long-time approximation (16) truncated to three terms. The time scale is set by taking $R=1$ and $D_\alpha=1$.

B. Exit time probability densities

Figure 2 shows the time dependence of the exit time probability density $q_\alpha(\mathbf{r},t)$ for a sphere, with $\alpha=2/3$ and $|\mathbf{r}|=0.25R$, for a perfectly absorbing boundary ($\Lambda=0$) and a partially absorbing boundary ($\Lambda=R$). The spectral decomposition (9) is compared to its short-time approximation (24) and long-time approximation (16), the latter being truncated to three terms. Both approximations are accurate in their ranges of applicability.

Figures 3–5 illustrate how the time dependence of the exit time probability density for a sphere varies with three relevant parameters: the exponent α, the starting point $\mathbf{r}$ and the length Λ. As expected, a decrease of α yields a broader probability density for the exit time, with a smaller typical time (the maximum is shifted to the left) (Fig. 3). When $r=|\mathbf{r}|/R$ increases, the starting point $\mathbf{r}$ becomes closer to the boundary, and the time needed to exit from the domain decreases. The probability density is thus shifted to smaller times (Fig. 4). Finally, an increase in Λ makes the boundary less permeable that increases the exit time. In this case, the exit time probability density is also getting broader (Fig. 5).

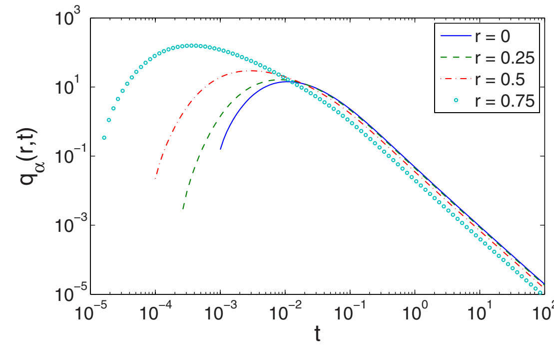

FIG. 4. (Color online) The exit time probability density $q_\alpha(\mathbf{r},t)$ for a sphere ($d=3$), with $\Lambda=0$, $\alpha=2/3$ and different values of $r=|\mathbf{r}|/R$. The time scale is set by taking $R=1$ and $D_\alpha=1$.

C. Rectangular domains

In order to justify the applicability of the asymptotic results for nonspherical domains, we also consider subdiffusion in a rectangular domain of size $b_x \times b_y$. Although the computations were realized for different rectangular domains, we only present the results for the unit square with $b_x=b_y=1$. As for rotation-invariant shapes, the Laplace operator eigenbasis is known explicitly,

$$u_{nk}(x,y) = u_n(x)u_k(y), \quad \lambda_{nk} = \lambda_n + \lambda_k,$$

where $u_n(x)$ and λ_n are the Laplace operator eigenfunctions and eigenvalues for the unit interval [66]. The computation of the exit time probability density through Eq. (9) is straightforward (technical details can be found in [40]).

Figure 6 shows the exit time probability density $q_\alpha(x,y,t)$ for the unit square $[0,1]\times[0,1]$, with $\alpha=2/3$, $x=0.2$, $y=0.4$ as an arbitrary example, and two values of Λ: $\Lambda=0$

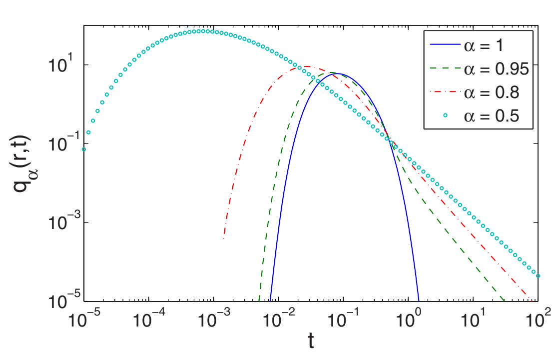

FIG. 3. (Color online) The exit time probability density $q_\alpha(\mathbf{r},t)$ for a sphere ($d=3$), with $\Lambda=0$, $|\mathbf{r}|=0.25R$ and different values of α. The time scale is set by taking $R=1$ and $D_\alpha=1$.

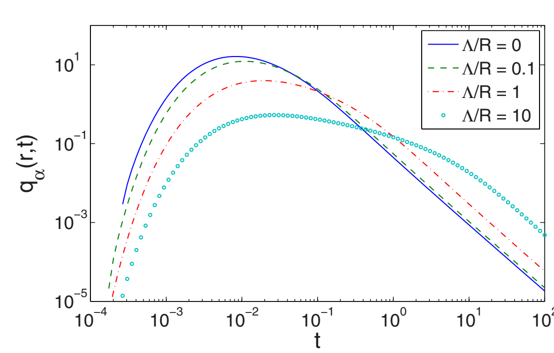

FIG. 5. (Color online) The exit time probability density $q_\alpha(\mathbf{r},t)$ for a sphere ($d=3$), with $\alpha=2/3$, $|\mathbf{r}|=0.25R$ and different values of Λ. The time scale is set by taking $R=1$ and $D_\alpha=1$.

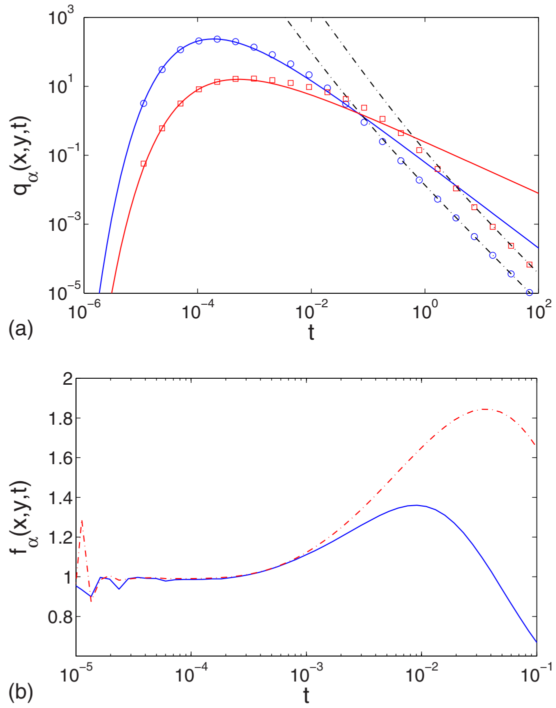

FIG. 6. (Color online) Top: The exit time probability density $q_\alpha(x,y,t)$ for the unit square $[0,1]\times[0,1]$, with $\alpha=2/3$, $x=0.2$, $y=0.4$, and two values of Λ: $\Lambda=0$ (blue circles) and $\Lambda=1$ (red squares). The time scale is set by taking $D_\alpha=1$. The solid lines show the short-time asymptotic formula (26) with $f_\alpha(x,y,t)=1$, the dash-dotted lines show the long-time asymptotic formula (16) that includes two terms. Bottom: the correction prefactor $f_\alpha(x,y,t)$ in Eq. (26). The solid blue line and the dash-dotted red line correspond to $\Lambda=0$ and $\Lambda=1$, respectively. Noisy variations around 1 at very small times are related to the computational inaccuracy of the spectral decomposition (see the text).

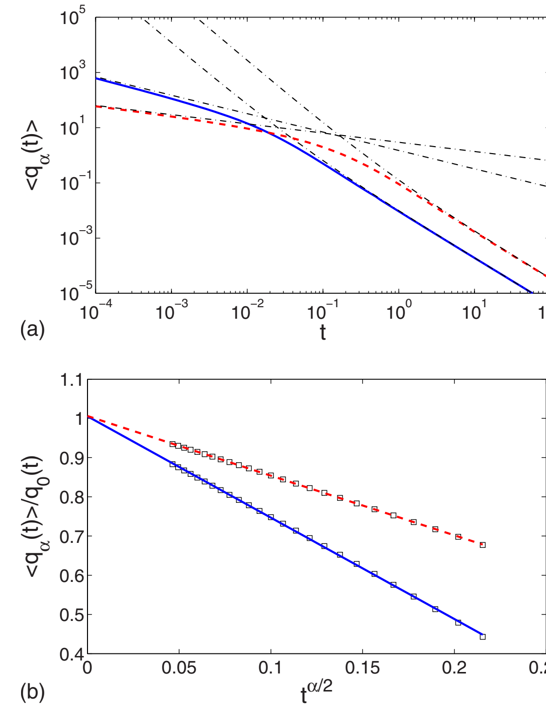

FIG. 7. (Color online) Top: The averaged exit time probability density $\langle q_\alpha(t)\rangle$ for the unit square $[0,1]\times[0,1]$, with $\alpha=2/3$, and two values of Λ: $\Lambda=0$ (solid blue line) and $\Lambda=1$ (dashed red line). The time scale is set by taking $D_\alpha=1$. The dash-dotted lines show the short-time and long-time asymptotic behaviors according to Eqs. (28) and (18), the latter including two terms. Bottom: The averaged exit time probability density $\langle q_\alpha(t)\rangle$ (shown by squares) which is normalized by the leading asymptotic term from Eq. (28), with $S/V=4$ for the unit square. The lines show a linear fit indicating the order of correction terms to Eq. (28).

(perfectly absorbing boundary) and $\Lambda=1$ (partially absorbing boundary). The asymptotic formulas (26) and (16) accurately describe the behavior of the density $q_\alpha(x,y,t)$ at short and long times, respectively. The bottom plot of Fig. 6 shows the correction function $f_\alpha(x,y,t)$ which is computed from Eq. (26). This function approaches 1 at short times. Noisy variations around this limit are related to the computational inaccuracy of the spectral decomposition (9) at very small times. In fact, one is trying to compute a very small probability $q_\alpha(x,y,t)$ by summing a very large number of terms which are slowly decreasing with m (roughly speaking, they are all in the order of 1). The round-off errors make such a computation inaccurate, and the spectral decomposition becomes useless at very small times. In turn, the asymptotic formula (26) is getting more and more accurate when the time decreases.

Note that when $x=y$ or $x=1-y$, the function $f_\alpha(x,y,t)$ is found to be approaching 2, while for $x=y=0.5$, it converges to 4. At short time, rare subdiffusing particles reaching the boundary most probably arrive at the nearest boundary points. For a general location of the starting point, there is only one nearest boundary point. When $x=y$ or $x=1-y$, there are two nearest points, while for $x=y=0.5$, there are four nearest points. Since the arrivals of subdiffusing particles on the boundary are rare events, they can be approximately considered as independent. The increase in chances for reaching the boundary is thus reflected in the supplementary factors 2 or 4 for the exit time probability density.

Similar reasoning may explain qualitatively the presence the factor $f_\alpha(\mathbf{r},t)=(|\mathbf{r}|/R)^{(1-d)/2}$ for rotation-invariant domains with $d>1$. When the starting point $\mathbf{r}$ approaches the origin ($|\mathbf{r}|$ goes to zero), the set of equidistance points from $\mathbf{r}$ (i.e., the sphere of radius $R-|\mathbf{r}|$ which is centered at $\mathbf{r}$) becomes closer and closer to the spherical domain (i.e., the sphere of radius R which is centered at 0). The consequent increase in the number of boundary points which can be reached by rare subdiffusing particles within a short time, is represented by increasing function $f_\alpha(\mathbf{r},t)$. When the particles start from the origin ($|\mathbf{r}|=0$), all the boundary points are equivalent that drastically changes the function $f_\alpha(\mathbf{r},t)$ according to Eq. (B2).

Figure 7 shows the averaged exit time probability density $\langle q_\alpha(t)\rangle$ for the unit square, with $\alpha=2/3$ as an arbitrary example, and two values of Λ: $\Lambda=0$ (perfectly absorbing boundary) and $\Lambda=1$ (partially absorbing boundary). The short- and long-time asymptotic formulas (28) and (18) are shown for comparison. As expected, the exponent of the power-law decay in the long-time limit is independent of Λ. The boundary permeability only affects the mean exit time

$\langle \tau_\Omega^{(1)} \rangle$ for normal diffusion which stands as a prefactor (a shift along the y axis on the logarithmic scale). In the short-time limit, Eq. (28) accurately describes the behavior of $\langle q_\alpha(t) \rangle$ with the exponents $\alpha/2-1$ for $\Lambda=0$ and $\alpha-1$ for $\Lambda=1$. On the bottom plot of Fig. 7, the density $\langle q_\alpha(t) \rangle$ is normalized by its asymptotic form according to Eq. (28). A linear dependence of this ratio on $t^{\alpha/2}$ explicitly gives the order of the leading correction term to Eq. (28), while its extrapolation to 1 as $t \to 0$ confirms the accuracy of the prefactor in Eq. (28). For instance, the leading correction term in the case $\Lambda=0$ is $t^{\alpha-1}$, and it diverges as t goes to 0 for $\alpha < 1$. Similar results were obtained for other rectangular domains (not presented). In particular, the presence of the surface-to-volume ratio in the short-time asymptotic formula (28) was confirmed.

V. CONCLUSION

The exit time of a subdiffusive process from a bounded domain with a partially absorbing/reflecting boundary was studied in detail. For an arbitrary bounded domain, an exact spectral decomposition was derived for the exit time probability density. Its asymptotic approximations in the short-time and long-time limits were investigated. A numerical computation confirmed the accuracy of these approximations. For rotation-invariant domains (e.g., a sphere), exact explicit formulas were given for the Laplace transform of the probability density. The long-time behavior of the probability density was governed by the moments of the exit time for normal diffusion. In the short-time limit, the exit time probability density which is averaged over uniformly chosen starting point, exhibited a power-law decay with the exponent $\alpha/2-1$ for a perfectly absorbing boundary ($\Lambda=0$) and the exponent $\alpha-1$ for a partially absorbing boundary ($\Lambda>0$). In the former case ($\Lambda=0$), the surface-to-volume ratio S/V can be extracted from fitting experimental data. In the latter case ($\Lambda>0$), the prefactor $(S/V)(D_\alpha/\Lambda)=W_\alpha S/V$ in Eq. (28) is independent of the diffusion coefficient D_α. Since particles can start infinitely close to the boundary, this is the permeability W_α which limits the transfer of particles in the short-time regime. This asymptotic behavior of $\langle q_\alpha(t) \rangle$ may potentially be used in order to determine the underlying surface permeability, reactivity or relaxivity from fitting experimental data.

It is worth noting that the assumption of a perfectly absorbing boundary is often not justified, and the consequent "choice" of the first relation in Eq. (28) may lead to erroneous determination of the exponent α and the surface-to-volume ratio. This observation is relevant for studies of subdiffusion inside a living cell with a semipermeable membrane, in a chemical reactor filled with catalytic grains of finite reactivity, or in mineral or biological samples which are probed by nuclear magnetic resonance measurements subject to surface relaxation.

ACKNOWLEDGMENT

The author thanks Professor J. Klafter for fruitful discussions. The work has been partly supported by the ANR program "DYOPTRI."

APPENDIX A: MOMENTS OF THE EXIT TIME FROM ROTATION-INVARIANT DOMAINS FOR NORMAL DIFFUSION

We calculate the moments $\tau_\Omega^{(k)}(\mathbf{r}) \equiv \mathbb{E}\{T_1^k\}$ of the exit time T_1 from a rotation-invariant domain for normal diffusion started from $\mathbf{r}$. The rotational invariance implies that $\tau_\Omega^{(k)}(\mathbf{r})$ is a function of the radial coordinate r so that Eqs. (12) become

$$\left(\frac{d^2}{dr^2} + \frac{d-1}{r}\frac{d}{dr}\right)\tau_\Omega^{(k)}(r) + \frac{k}{D_1}\tau_\Omega^{(k-1)}(r) = 0, \tag{A1}$$

$$\Lambda\left(\frac{d}{dr}\tau_\Omega^{(k)}(r)\right)_{r=R} + \tau_\Omega^{(k)}(R) = 0. \tag{A2}$$

A solution of these equations is searched in the form

$$\tau_\Omega^{(k)}(r) = k!\,\tau_0^k \sum_{j=0}^{k} a_j^{(k)} (r/R)^{2j},$$

where $\tau_0 = R^2/D_1$ is a diffusion time scale, and $a_j^{(k)}$ are unknown coefficients to be determined. The substitution of this form into Eq. (A1) yields a set of recurrent relations for the coefficients $a_j^{(k)}$,

$$a_j^{(k)} = -\frac{a_{j-1}^{(k-1)}}{2j(2j+d-2)} \quad (j=1\ldots k).$$

Applying repeatedly this relation, one gets

$$a_j^{(k)} = b_j a_0^{(k-j)} \quad (j=1\ldots k),$$

where

$$b_j \equiv \begin{cases} \dfrac{(-1)^j}{2^j j!\, d(d+2)\ldots[d+2(j-1)]} & (j>0), \\ 1 & (j=0). \end{cases}$$

In turn, Eq. (A2) implies

$$a_0^{(k)} = -\sum_{j=1}^{k} (2j\Lambda/R+1) a_j^{(k)} = -\sum_{j=1}^{k} (2j\Lambda/R+1) b_j a_0^{(k-j)}.$$

Since $\tau_\Omega^{(0)}(\mathbf{r})=1$, the initial relation $a_j^{(0)}=\delta_{j,0}$ allows one to solve the above set of linear equations which can also be rewritten as

$$\sum_{j=0}^{k-1} c_j a_0^{(k-j)} = -c_k, \tag{A3}$$

where $c_j=(2j\Lambda/R+1)b_j$ $(j=0\ldots k)$. A recursive computation or a matrix inversion are efficient ways for finding a numerical solution of this system. Given the particular structure of these equations, the following explicit solution can also be derived,

$$a_0^{(k)} = \sum_{\substack{i_1+\ldots+ki_k=k,\\ i_1\ge 0\ldots i_k\ge 0}} (-1)^{i_1+\ldots+i_k} \frac{(i_1+\ldots+i_k)!}{i_1!\ldots i_k!} c_1^{i_1}\ldots c_k^{i_k}.$$

For instance, one has

$$a_0^{(1)} = -c_1,$$

$$a_0^{(2)} = -c_2 + c_1^2,$$

$$a_0^{(3)} = -c_3 + 2c_1c_2 - c_1^3,$$

$$a_0^{(4)} = -c_4 + 2c_1c_3 - 3c_1^2c_2 + c_2^2 + c_1^4.$$

The kth moment of the exit time is therefore

$$\tau_\Omega^{(k)}(\mathbf{r}) = k!\left(\frac{R^2}{D_1}\right)^k \sum_{j=0}^{k} b_j a_0^{(k-j)}(|\mathbf{r}|/R)^{2j}. \tag{A4}$$

Taking $\mathbf{r}=0$, we find

$$\tau_\Omega^{(k)}(0) = k!\left(\frac{R^2}{D_1}\right)^k a_0^{(k)}$$

that gives a physical interpretation for the coefficients $a_0^{(k)}$. If the starting point is uniformly distributed over the domain, one gets

$$\langle \tau_\Omega^{(k)} \rangle \equiv \frac{1}{V}\int_\Omega d\mathbf{r}\, \tau_\Omega^{(k)}(\mathbf{r}) = k!d\left(\frac{R^2}{D_1}\right)^k \sum_{j=0}^{k} \frac{b_j a_0^{(k-j)}}{2j+d}.$$

APPENDIX B: SHORT-TIME ASYMPTOTIC BEHAVIOR OF THE EXIT TIME PROBABILITY DENSITY

In Sec. III A, we considered the short-time asymptotic behavior of the exit time probability density $q_\alpha(\mathbf{r},t)$ and derived the asymptotic results (23) and (24) in the case $|\mathbf{r}|>0$. Both equations (23) and (24) formally diverge at $|\mathbf{r}|=0$, although this point might seem to be "ordinary" from a probabilistic point of view. In this Section, we clarify this "paradox."

The analysis relies on the asymptotic behavior of the Laplace transform $\tilde{q}_\alpha(\mathbf{r},s)$ from Eq. (21) as s goes to infinity. In this limit, one gets $R\sqrt{s^\alpha/D_\alpha} \gg 1$ so that Eq. (22) becomes

$$W_d(s) \simeq \frac{e^{R\sqrt{s^\alpha/D_\alpha}}}{\sqrt{4\pi}(R^2s^\alpha/(4D_\alpha))^{1/4}}\left(1 + \frac{1-d^2}{8}\frac{\Lambda}{R} + \Lambda\sqrt{s^\alpha/D_\alpha}\right).$$

If $|\mathbf{r}|\sqrt{s^\alpha/D_\alpha} \gg 1$, one derives Eq. (23).

However, if $|\mathbf{r}|=0$ (or very small), the condition $|\mathbf{r}|\sqrt{s^\alpha/D_\alpha} \gg 1$ cannot be satisfied. In this case, Eq. (21) becomes

$$\tilde{q}_\alpha(0,s) = \frac{1}{\Gamma(d/2)W_d(s)}\left(\frac{R^2s^\alpha}{4D_\alpha}\right)^{(d-2)/4}.$$

The above asymptotic formula for $W_d(s)$ then yields

$$\tilde{q}_\alpha(0,s) \simeq \frac{\sqrt{4\pi}}{\Gamma(d/2)}\left(\frac{R^2s^\alpha}{4D_\alpha}\right)^{(d-1)/4} \frac{e^{-R\sqrt{s^\alpha/D_\alpha}}}{1 + \frac{1-d^2}{8}\frac{\Lambda}{R} + \Lambda\sqrt{s^\alpha/D_\alpha}}$$

for $s\to\infty$. Using Eq. (C5) from Appendix C, we deduce the short-time asymptotic behavior of the probability density $q_\alpha(0,t)$ for a perfectly absorbing boundary ($\Lambda=0$) and for a partially absorbing boundary ($\Lambda>0$)

$$q_\alpha(0,t) \simeq \frac{2t^{-1}}{\Gamma(d/2)\sqrt{2-\alpha}}\exp\left[-(2-\alpha)\left(\frac{R^2\alpha^\alpha}{4D_\alpha t^\alpha}\right)^{1/(2-\alpha)}\right] \times \begin{cases} \alpha^{1/2}\left(\dfrac{R^2\alpha^\alpha}{4D_\alpha t^\alpha}\right)^{d/[2(2-\alpha)]} & (\Lambda=0), \\ \alpha^{(1-\alpha)/2}\left(\dfrac{R^2\alpha^\alpha}{4D_\alpha t^\alpha}\right)^{(d-\alpha)/[2(2-\alpha)]}\dfrac{\sqrt{D_\alpha t^\alpha}}{\Lambda} & (\Lambda>0). \end{cases} \tag{B1}$$

A comparison with the asymptotic formula (26) yields the correction prefactor $f_\alpha(\mathbf{r},t)$

$$f_\alpha(0,t) \simeq \frac{2\sqrt{\pi}}{\Gamma(d/2)}\left(\frac{R^2\alpha^\alpha}{4D_\alpha t^\alpha}\right)^{(d-1)/[2(2-\alpha)]} \tag{B2}$$

that provides an explicit example of a power-law dependence of $f_\alpha(\mathbf{r},t)$ on time. As we already mentioned in Sec. IV C, the point $\mathbf{r}=0$ is indeed special in the short-time limit because all the boundary points are equidistant from the origin. This leads to an abrupt change of the function $f_\alpha(\mathbf{r},t)$ from $(|\mathbf{r}|/R)^{(1-d)/2}$ to Eq. (B2).

This situation can be illustrated in the case $d=1$, for which Eqs. (24) and (B1) yield $f_\alpha(x,t)\simeq 1$ ($x>0$) and $f_\alpha(0,t)\simeq 2$. How is it possible that the probability density $q_\alpha(\mathbf{r},t)$ follows Eq. (24) for any $|\mathbf{r}|>0$ and then "jumps" abruptly to a twice higher value at $|\mathbf{r}|=0$? The explanation is actually simple. For $d=1$, the explicit form of $\tilde{q}_\alpha(\mathbf{r},s)$ yields as $s\to\infty$

$$\tilde{q}_\alpha(\mathbf{r},s) \simeq \frac{e^{-(R-|\mathbf{r}|)\sqrt{s^\alpha/D_\alpha}} + e^{-(R+|\mathbf{r}|)\sqrt{s^\alpha/D_\alpha}}}{1+\Lambda\sqrt{s^\alpha/D_\alpha}}.$$

When $|\mathbf{r}|>0$, the second exponential term becomes less and less significant, in comparison to the first one, as s increases. In the limit $s\to\infty$, the second term can be neglected, and one retrieves Eq. (23). When $|\mathbf{r}|=0$, the two terms are identical that gives the supplementary factor 2 in Eq. (B1). For small $|\mathbf{r}|$, there is an intermediate region of values s for which the two terms are relevant. If we keep these two terms, the short-time asymptotic behavior is

$$q_\alpha(\mathbf{r},t) \simeq t^{-1}\left\{ q_\alpha^{(0)}\left(\left[\frac{(R-|\mathbf{r}|)^2\alpha^\alpha}{4D_\alpha t^\alpha}\right]^{1/(2-\alpha)}, \frac{\sqrt{D_\alpha t^\alpha}}{\Lambda}\right) + q_\alpha^{(0)}\left(\left[\frac{(R+|\mathbf{r}|)^2\alpha^\alpha}{4D_\alpha t^\alpha}\right]^{1/(2-\alpha)}, \frac{\sqrt{D_\alpha t^\alpha}}{\Lambda}\right)\right\}.$$

APPENDIX C: FREE SUBDIFFUSIVE PROPAGATOR

The properties of the free subdiffusive propagator $G_t^{\alpha,\mathrm{free}}(\mathbf{r}_0,\mathbf{r})$ for the whole space $\mathbb{R}^d$ have been reported in the literature (e.g., see [67–69]). We summarize several relations which are useful for studying the asymptotic behavior of the exit time probability density.

The Laplace transform $\mathcal{L}$ in time t and the Fourier transform $\mathcal{F}$ in position $\mathbf{r}$ reduce Eqs. (1) and (3) to a linear equation which has an exact explicit solution,

$$\mathcal{F}\{\mathcal{L}[G_t^{\alpha,\mathrm{free}}(\mathbf{r}_0,\mathbf{r})](s)\}(\mathbf{k}) = e^{-i\mathbf{k}\mathbf{r}_0}\frac{s^{\alpha-1}}{s^\alpha + D_\alpha|\mathbf{k}|^2}.$$

The inverse Fourier transform of this function is

$$\mathcal{L}[G_t^{\alpha,\mathrm{free}}(\mathbf{r}_0,\mathbf{r})](s) = \frac{1}{(2\pi)^{d/2}} s^{-1}(s^\alpha/D_\alpha)^{d/2}\frac{K_{d/2-1}\left(r\sqrt{s^\alpha/D_\alpha}\right)}{\left(r\sqrt{s^\alpha/D_\alpha}\right)^{d/2-1}}, \tag{C1}$$

where $K_\nu(z)$ is the modified Bessel function of the second kind, and $r=|\mathbf{r}-\mathbf{r}_0|$ is the distance between points $\mathbf{r}$ and $\mathbf{r}_0$. It may be useful to rewrite this formula explicitly for $d=1,2,3$,

$$\mathcal{L}[G_t^{\alpha,\mathrm{free}}(\mathbf{r}_0,\mathbf{r})](s) = \begin{cases} \dfrac{s^{\alpha/2-1}}{2\sqrt{D_\alpha}}\exp(-r\sqrt{s^\alpha/D_\alpha}), \\ \dfrac{s^{\alpha-1}}{2\pi D_\alpha}K_0(r\sqrt{s^\alpha/D_\alpha}), \\ \dfrac{s^{\alpha-1}}{4\pi D_\alpha r}\exp(-r\sqrt{s^\alpha/D_\alpha}). \end{cases} \tag{C2}$$

The subdiffusive propagator $G_t^{\alpha,\mathrm{free}}(\mathbf{r}_0,\mathbf{r})$ is formally obtained by the inverse Laplace transform of the right-hand side in Eq. (C1) which can be expressed in terms of a Fox H-function [70]. For practical purposes, explicit asymptotic behaviors at short and long times are often more appropriate than using a formal solution with H-functions. The long-time behavior corresponds to the limit of $\mathcal{L}[G_t^{\alpha,\mathrm{free}}(\mathbf{r}_0,\mathbf{r})](s)$ as s goes to 0. It can be obtained from a Taylor series expansion of the modified Bessel function and term-by-term computation of the inverse Laplace transforms of powers of s.

The short-time behavior of the free subdiffusive propagator corresponds to the limit of $\mathcal{L}[G_t^{\alpha,\mathrm{free}}(\mathbf{r}_0,\mathbf{r})](s)$ as s goes to infinity. In this limit, Eq. (C1) becomes

$$\mathcal{L}[G_t^{\alpha,\mathrm{free}}(\mathbf{r}_0,\mathbf{r})](s) \simeq \frac{s^{-1}}{2(2\pi)^{(d-1)/2}}\left(\frac{s^\alpha}{D_\alpha}\right)^{(d+1)/4}\frac{e^{-r\sqrt{s^\alpha/D_\alpha}}}{r^{(d-1)/2}}. \tag{C3}$$

The Laplace method (or, more generally, the saddle-point method) [48] allows one to derive the asymptotic behavior (C4) of the function $\mathcal{L}[t^{-\gamma}e^{-c/t^\beta}](s)$ as s goes to infinity (here β, γ and $c>0$ are fixed numbers). Substitution of β, γ and c by new parameters α, κ and r leads to another form (C5) of the same relation. A comparison of this form to Eq. (C3) suggests to take $\kappa=(d+1)/4-1$ in order to derive the short-time asymptotic behavior (C6) of the free subdiffusive propagator.

$$\mathcal{L}[t^{-\gamma}e^{-c/t^\beta}](s) \simeq \sqrt{\frac{2\pi}{\beta+1}}(\beta c)^{(1-2\gamma)/[2(\beta+1)]}s^{(2\gamma-\beta-2)/[2(\beta+1)]}\exp[-s^{\beta/(\beta+1)}c^{1/(\beta+1)}(\beta^{1/(\beta+1)}+\beta^{-\beta/(\beta+1)})]. \tag{C4}$$

$$\mathcal{L}^{-1}[s^\kappa e^{-r\sqrt{s^\alpha/D_\alpha}}](t) \simeq \frac{\alpha^{\kappa+1/2}}{\sqrt{\pi(2-\alpha)}}\left(\frac{r^2\alpha^\alpha}{4D_\alpha t^\alpha}\right)^{(\kappa+1/2)/(2-\alpha)}t^{-(\kappa+1)}\exp\left[-(2-\alpha)\left(\frac{r^2\alpha^\alpha}{4D_\alpha t^\alpha}\right)^{1/(2-\alpha)}\right]. \tag{C5}$$

$$G_t^{\alpha,\mathrm{free}}(\mathbf{r}_0,\mathbf{r}) \simeq \frac{\alpha^{(d\alpha-1)/2}}{\sqrt{2-\alpha}}(4\pi D_\alpha t^\alpha)^{-d/2}\left(\frac{|\mathbf{r}-\mathbf{r}_0|^2\alpha^\alpha}{4D_\alpha t^\alpha}\right)^{-d(1-\alpha)/[2(2-\alpha)]}\exp\left[-(2-\alpha)\left(\frac{|\mathbf{r}-\mathbf{r}_0|^2\alpha^\alpha}{4D_\alpha t^\alpha}\right)^{1/(2-\alpha)}\right]. \tag{C6}$$

For completeness, we note that the inverse Laplace transform $\mathcal{L}^{-1}[s^\kappa e^{-r\sqrt{s^\alpha/D_\alpha}}](t)$ can be written exactly in the form of a series [71]

$$\mathcal{L}^{-1}\left[s^\kappa e^{-r\sqrt{s^\alpha/D_\alpha}}\right](t) = -\frac{1}{\pi t^{1+\kappa}}\sum_{n=0}^{\infty}\frac{\sin[\pi(\kappa+n\alpha/2)]\Gamma(1+\kappa+n\alpha/2)}{n!} \times\left(-\frac{\sqrt{D_\alpha t^\alpha}}{r}\right)^{-n}.$$

However, this representation is only efficient in the long-time limit.

Several comments are in order:

(i) For normal diffusion ($\alpha=1$), Eq. (C6) is reduced to the Gaussian propagator

$$G_t^{1,\mathrm{free}}(\mathbf{r}_0,\mathbf{r}) = \frac{1}{(4\pi D_1 t)^{d/2}}\exp\left[-\frac{|\mathbf{r}-\mathbf{r}_0|^2}{4D_1 t}\right],$$

which is applicable for any time t (not only in the short-time limit).

(ii) When $\alpha<1$, the stretched-exponential behavior (C6) is not exact, but approximate for short times. Note that correction terms in fractional powers of t may be significant if t is not small enough.

(iii) The asymptotic result (C6) is derived for fixed $\mathbf{r}_0$ and $\mathbf{r}$. When $\mathbf{r}$ approaches $\mathbf{r}_0$, the subdiffusive propagator diverges, in contrast to the case of normal diffusion. Note that the exact Eqs. (C2) also diverge as $\mathbf{r}$ approaching $\mathbf{r}_0$ (or $r\to 0$) for $d=2$ and $d=3$ *even* for normal diffusion ($\alpha=1$). These issues were already discussed in the literature (e.g., see [54]).

(iv) The free propagator for subdiffusion on a line, in half-space and in a box, as well as the related boundary value problems were studied by Metzler and Klafter [69]. In particular, they discussed the representation of the propagator in terms of Fox-functions and the short-time asymptotic behavior [Eq. (C6)] for $d=1$.

(v) The approximate formula (C6) reaches a maximum at time t_0 which may serve as an appropriate time scale

$$t_0 = \alpha\left(\frac{2(2-\alpha)}{d}\right)^{(2-\alpha)/\alpha}\left(\frac{|\mathbf{r}-\mathbf{r}_0|^2}{4D_\alpha}\right)^{1/\alpha}. \qquad \text{(C7)}$$

This time scale was used for plotting Fig. 1.

(vi) In the short-time limit, particles have no enough time for exploring the space so that a subdiffusive propagator for a bounded domain can be approximated by that for the whole space. Eq. (C6) provides therefore the short-time asymptotic behavior for a general spectral decomposition (if the both points $\mathbf{r}_0$ and $\mathbf{r}$ are not close to the boundary)

$$\sum_{m=0}^{\infty} E_\alpha(-D_\alpha\lambda_m t^\alpha)u_m^*(\mathbf{r}_0)u_m(\mathbf{r}) \simeq G_t^{\alpha,\mathrm{free}}(\mathbf{r}_0,\mathbf{r}). \qquad \text{(C8)}$$

(vii) This relation is useful for theoretical and numerical computations at short times because a slow convergence may prohibit using spectral decompositions.

(viii) As a corollary, one can calculate the probability for a particle to be found at time t inside a sphere of radius R around the starting point

$$P(R,t) \equiv \int_{\{\mathbf{r}\in\mathbb{R}^d:|\mathbf{r}|<R\}} d\mathbf{r}\, G_t^{\alpha,\mathrm{free}}(0,\mathbf{r}).$$

In the short-time limit, the use of Eq. (C6) yields

$$P(R,t) \simeq 1 - \frac{1}{\Gamma(d/2)\sqrt{\alpha(2-\alpha)}}\left(\frac{R^2\alpha^\alpha}{4D_\alpha t^\alpha}\right)^{(d-2)/[2(2-\alpha)]} \times \exp\left[-(2-\alpha)\left(\frac{R^2\alpha^\alpha}{4D_\alpha t^\alpha}\right)^{1/(2-\alpha)}\right].$$

Note that this probability is different from the survival probability for a sphere because particles can leave the sphere and then return to it up to time t.

[1] M. Weiss, M. Elsner, F. Kartberg, and T. Nilsson, Biophys. J. **87**, 3518 (2004).
[2] I. Golding and E. C. Cox, Phys. Rev. Lett. **96**, 098102 (2006).
[3] B. Berkowitz, J. Klafter, R. Metzler, and H. Scher, Water Resour. Res. **38**, 1191 (2002).
[4] J.-P. Bouchaud and A. Georges, Phys. Rep. **195**, 127 (1990).
[5] R. Metzler and J. Klafter, Phys. Rep. **339**, 1 (2000).
[6] G. M. Zaslavsky, Phys. Rep. **371**, 461 (2002).
[7] S. Havlin and D. ben Avraham, Adv. Phys. **51**, 187 (2002).
[8] R. Kimmich, Chem. Phys. **284**, 253 (2002).
[9] R. Metzler and J. Klafter, J. Phys. A **37**, R161 (2004).
[10] T. Kosztołowicz, K. Dworecki, and S. Mrówczyński, Phys. Rev. Lett. **94**, 170602 (2005).
[11] B. Alberts, D. Bray, J. Lewis, M. Raff, K. Roberts, and J. D. Watson, *Molecular Biology of the Cell*, 3rd ed. (Garland, New York, 1994).
[12] J. M. Schurr, Biophys. J. **10**, 717 (1970).
[13] D. Shoup and A. Szabo, Biophys. J. **40**, 33 (1982).
[14] F. C. Collins and G. E. Kimball, J. Colloid Sci. **4**, 425 (1949).
[15] G. Wilemski and M. Fixman, J. Chem. Phys. **58**, 4009 (1973).
[16] A. Szabo, K. Schulten, and Z. Schulten, J. Chem. Phys. **72**, 4350 (1980).
[17] G. H. Weiss, J. Stat. Phys. **42**, 3 (1986).
[18] D. Holcman and Z. Schuss, J. Chem. Phys. **122**, 114710 (2005).
[19] K. R. Brownstein and C. E. Tarr, Phys. Rev. A **19**, 2446 (1979).
[20] S. Redner, *A Guide to First-Passage Processes* (Cambridge University Press, Cambridge, England, 2001).
[21] B. D. Hughes, *Random Walks and Random Environments* (Clarendon Press, Oxford, 1995).
[22] D. Holcman, A. Marchewka, and Z. Schuss, Phys. Rev. E **72**, 031910 (2005).
[23] P. Levitz, D. S. Grebenkov, M. Zinsmeister, K. M. Kolwankar, and B. Sapoval, Phys. Rev. Lett. **96**, 180601 (2006).
[24] S. Condamin, O. Bénichou, and M. Moreau, Phys. Rev. Lett. **95**, 260601 (2005).
[25] S. Condamin, O. Bénichou, and M. Moreau, Phys. Rev. E **72**, 016127 (2005).
[26] S. Condamin, O. Bénichou, V. Tejedor, R. Voituriez, and J. Klafter, Nature (London) **450**, 77 (2007).
[27] D. S. Grebenkov, Phys. Rev. E **76**, 041139 (2007).
[28] R. C. Lua and A. Y. Grosberg, Phys. Rev. E **72**, 061918 (2005).
[29] S. B. Yuste and K. Lindenberg, Phys. Rev. E **76**, 051114 (2007).
[30] S. Condamin, O. Bénichou, and J. Klafter, Phys. Rev. Lett. **98**, 250602 (2007).
[31] S. Condamin, V. Tejedor, R. Voituriez, O. Bénichou, and J. Klafter, Proc. Natl. Acad. Sci. U.S.A. **105**, 5675 (2008).
[32] B. Sapoval, Phys. Rev. Lett. **73**, 3314 (1994).
[33] D. S. Grebenkov, *Focus on Probability Theory*, edited by L. R. Velle (Hauppauge: Nova Science Publishers, New York, 2006), pp. 135–169.
[34] A. Singer, Z. Schuss, A. Osipov, and D. Holcman, SIAM J. Appl. Math. **68**, 844 (2008).
[35] D. S. Grebenkov, M. Filoche, and B. Sapoval, Phys. Rev. E **73**, 021103 (2006).
[36] M. Filoche and B. Sapoval, Eur. Phys. J. B **9**, 755 (1999).
[37] D. S. Grebenkov, M. Filoche, and B. Sapoval, Eur. Phys. J. B **36**, 221 (2003).
[38] M. Felici, M. Filoche, C. Straus, T. Similowski, and B. Sapoval, Respir. Physiol. Neurbiol. **145**, 279 (2005).
[39] D. S. Grebenkov, Fractals **14**, 231 (2006).
[40] D. S. Grebenkov, Rev. Mod. Phys. **79**, 1077 (2007).
[41] S. G. Samko, A. A. Kilbas, and O. I. Marichev, *Fractional*

Integrals and Derivatives: Theory and Applications (Gordon and Breach Science Publishers, Amsterdam, 1993).
[42] A. A. Kilbas, H. M. Srivastava, and J. J. Trujillo, *Theory and Applications of Fractional Differential Equations*, Series “Mathematics Studies” (Elsevier, Amsterdam, 2006), Vol. 204.
[43] K. Seki, M. Wojcik, and M. Tachiya, J. Chem. Phys. **119**, 2165 (2003).
[44] J. D. Eaves and D. R. Reichman, J. Phys. Chem. B **112**, 4283 (2008).
[45] J. Sung and R. J. Silbey, Phys. Rev. Lett. **91**, 160601 (2003).
[46] M. A. Lomholt, I. M. Zaid, and R. Metzler, Phys. Rev. Lett. **98**, 200603 (2007).
[47] T. Chou and M. R. D’Orsogna, J. Chem. Phys. **127**, 105101 (2007).
[48] R. Courant and D. Hilbert, *Methods of Mathematical Physics* (Wiley, New York, 1937–1989), Vol. I.
[49] F. Mainardi and R. Gorenflo, J. Comput. Appl. Math. **118**, 283 (2000).
[50] S. Bochner, Proc. Natl. Acad. Sci. U.S.A. **35**, 368 (1949).
[51] W. Feller, *An Introduction to Probability Theory and Its Applications*, 3rd ed. (Wiley, New York, 1968).
[52] I. M. Sokolov, Phys. Rev. E **63**, 011104 (2000).
[53] E. Barkai, R. Metzler, and J. Klafter, Phys. Rev. E **61**, 132 (2000).
[54] E. Barkai, Phys. Rev. E **63**, 046118 (2001).
[55] M. M. Meerschaert and H.-P. Scheffler, J. Appl. Probab. **41**, 623 (2004).
[56] H. Risken, *The Fokker-Planck Equation: Methods of Solution and Applications*, 3rd ed. (Springer, Berlin, 1996).
[57] A. N. Borodin and P. Salminen, *Handbook of Brownian Motion: Facts and Formulae* (Birkhauser Verlag, Basel, Boston, Berlin, 1996).
[58] M. E. Muller, Ann. Math. Stat. **27**, 569 (1956).
[59] L. H. Zheng and Y. C. Chiew, J. Chem. Phys. **90**, 322 (1989).
[60] S. B. Lee, I. C. Kim, C. A. Miller, and S. Torquato, Phys. Rev. B **39**, 11833 (1989).
[61] D. S. Grebenkov, Phys. Rev. Lett. **95**, 200602 (2005).
[62] D. S. Grebenkov, A. A. Lebedev, M. Filoche, and B. Sapoval, Phys. Rev. E **71**, 056121 (2005).
[63] D. S. Grebenkov, Diff. Fundam. **5**, 1 (2007).
[64] D. S. Grebenkov, J. Chem. Phys. **132**, 034104 (2010)
[65] H. S. Carslaw and J. C. Jaeger, *Conduction of Heat in Solids*, 2nd ed. (Clarendon, Oxford, 1959).
[66] J. Crank, *The Mathematics of Diffusion*, 2nd ed. (Clarendon, Oxford, 1975).
[67] H. Weissman, G. H. Weiss, and S. Havlin, J. Stat. Phys. **57**, 301 (1989).
[68] J. Klafter and G. Zumofen, J. Phys. Chem. **98**, 7366 (1994).
[69] R. Metzler and J. Klafter, Physica A **278**, 107 (2000).
[70] F. Mainardi, G. Pagnini, and R. K. Saxena, J. Comput. Appl. Math. **178**, 321 (2005).
[71] T. Kosztołowicz, J. Phys. A **37**, 10779 (2004).